J. Phys. C: Solid State Phys. **19** (1986) 3325–3341. Printed in Great Britain

A simulation study of the disordered phase of CBr_4: I. Single-particle properties

Martin T Dove

Department of Theoretical Chemistry, University Chemical Laboratories, Lensfield Road, Cambridge CB2 1EW, UK

Received 14 October 1985

Abstract. The orientationally disordered phase of carbon tetrabromide at 345 K has been studied using the molecular dynamics simulation technique. A realistic inter-molecular potential has been developed, which was parametrised by fitting to some experimental data and tested by comparing the results of the simulations with other independent experimental data. This model has been used to study various properties generally associated with the behaviour of single molecules and their neighbouring molecules: thermodynamic properties, the orientational order of single molecules, correlations between the orientations of neighbouring molecules, and single-molecule dynamics. The results are compared with previous work, and it is shown that the molecular orientations are more uniform and their dynamics more complicated than previously thought.

1. Introduction

The study of disorder within crystalline media is one that has revealed a rich diversity of phenomena. One form of disorder is orientational disorder (OD) within molecular crystals (Sherwood 1979), and carbon tetrabromide might be considered to be prototypical of this class of materials. In general, three-dimensional OD crystals are composed of small highly symmetrical molecules (e.g. dumb-bells, tetrahedra or octahedra) with only weak anisotropic inter-molecular potentials. Thus the long-range ordering of the positions of the molecules is largely independent of the fine details of the intermolecular potential, so the positional ordering is often of high symmetry (e.g. cubic or hexagonal) with the molecules lying on sites with higher symmetry than the molecular symmetry. In many systems it is this difference between the site and molecular symmetries that effectively defines the orientational disorder. The anisotropic orientational interactions may only affect the short-range motions, but nevertheless can be crucial in determining the dynamical behaviour of these systems.

One aspect of the inter-molecular forces that partly determines the behaviour of the disorder is the relative size of the static crystal field and the kinetic energy. For varying ratios of these contributions to the Hamiltonian the orientational motions of the molecules range from free rotation and complete disorder (e.g. CH_4, H_2) via rotational diffusion in an anisotropic potential (e.g. SF_6) to rotational jumps between well defined potential wells (e.g. NH_4Cl), the latter case being similar to an Ising model, with the

0022-3719/86/183325 + 17 $02.50

orientations being described in terms of spin variables. This variation has been described by Huller and Press (1979).

There are a number of experimental approaches to the study of OD crystals. Diffraction studies can yield an approximate form of the molecular orientational distribution function (e.g., Dolling *et al* 1979); nuclear resonance methods and quasi-elastic incoherent neutron scattering can give reorientational relaxation times; inelastic coherent neutron and light scattering studies can probe the collective excitations. Moreover, combinations of techniques can give information concerning single-molecule potentials (Press 1981). More recently computer simulation techniques have been applied to the study of OD crystals, particularly the method of molecular dynamics simulation (MDS) (Pawley and Dove 1983). The value of this approach is that unambiguous information can readily be extracted, which may not be possible with experiments. Also simulation studies can be profitably used in the analysis of experimental data. Thus the technique of MDS has been successfully applied to provide an understanding of the origin and nature of the disorder in SF_6 (Dove and Pawley 1983, 1984, Dove *et al* 1986a, b), and has been used to assess the theories of rotation–translation coupling in NaCN and $NaNO_2$ (Lynden-Bell *et al* 1983, 1984).

As stated above, CBr_4 is representative of OD crystals, and for this reason we have chosen it for a study using MDS. The overall aim is to study the phenomenon of rotation–translation coupling in this material, but that aspect of this work is reserved for the following paper (Dove and Lynden-Bell 1986). In the present paper we have three aims. The first is to develop a model inter-molecular potential for CBr_4 that will reproduce, as closely as is practicable, the behaviour found in the real OD phase of CBr_4, and which can be used to obtain useful information about the disorder. The second aim is to understand the nature of the disorder along the lines outlined above in the discussion of the inter-relation between crystal field and kinetic energy, considering both the orientational order and rotational dynamics. Thirdly, we explore the effects of varying the anisotropy of the inter-molecular orientational potential.

2. Previous results

The OD phase of CBr_4 is face-centred cubic, and exists over the temperature range of 320 K to the melting point at 365 K. The C–Br bond orientational distribution function (ODF) was studied by neutron scattering by Dolling *et al* (1979) and More *et al* (1980), using a Kubic harmonic expansion formalism for the ODF. The data for the latter study were re-analysed by Press *et al* (1979), extending the Kubic harmonic formalism to include coupling of the molecular orientations to the centre-of-mass displacements. The resultant ODF is close to that expected for a uniform distribution of orientations, with the only significant feature being a broad peak along the 110 direction.

The low-temperature ordered phase is monoclinic, with space group $C2/c$ (More *et al* 1977). This structure has 32 molecules in the unit cell, with four independent molecules in the asymmetric unit. More *et al* (1977) have shown how the centre-of-mass structures of the two phases are related, the monoclinic structure being close to a pseudo-cubic structure. In the low-temperature phase all the molecules have orientations that are close to a D_{2d} orientation of a tetrahedron in an octahedral site (see § 4). There are six possible such orientations, which have the C–Br bonds lying only 9.7° away from the 110 directions. As this would give a bond ODF similar in structure to that observed in the OD phase, it has been suggested (More *et al* 1980) and assumed (Coulon and Descamps

1980) that the OD phase has the molecules all oriented in D_{2d} orientations but with the particular orientation (out of the six possible) random. This forms the basis of a discrete spin model of the disorder. Because of steric hindrance effects arising from the short-range repulsive forces that occur when the electronic wavefunctions of two anisotropic molecules overlap not all possible relative orientations of neighbouring molecules would be possible in this model, and these resulting short-range orientational correlations have been used to explain anomalous diffuse scattering observed in the OD phase (Coulon and Descamps 1980).

Aspects of the dynamics have been studied by coherent inelastic neutron scattering (More and Fouret 1980, More *et al* 1984). No librational modes were observed, and scattering from acoustic modes broadened and weakened with increasing phonon wavevector. In addition, quasi-elastic scattering was measured at several momentum transfers.

3. Details of the simulation

For our computer simulations we used the same techniques as were used in corresponding simulations of SF_6 (Pawley and Dove 1983, Dove and Pawley 1983, 1984). The simulation calculations were performed on the ICL distributed array processor (DAP) at Queen Mary College, using a modified version of the program used for SF_6 (Pawley and Thomas 1982a). The MDS sample consisted of 4096 molecules initially arranged on an FCC lattice, the sample being approximately cubic with skew-periodic boundary conditions. The architecture of the DAP is a 64×64 square grid of separate processing elements, with connections between neighbouring processing elements and with periodic boundary connections. The three-dimensional sample was mapped onto the DAP hardware in a manner similar to that described by Pawley and Thomas (1982b), by considering the DAP to be a long vector of 4096 elements. In order to produce a near-cubic shape of our sample, we had to treat the long vector of the DAP as a crinkled vector. This is illustrated in figure 1; for more details the reader is referred to the paper by Pawley and Thomas (1982b). With this mapping, the shape of the MDS sample is defined by the three vectors

$$\boldsymbol{X} = (10, -1, 0)a \qquad \boldsymbol{Y} = (-2, 10.5, -0.5)a \qquad \boldsymbol{Z} = (-2, -1, 10)a$$

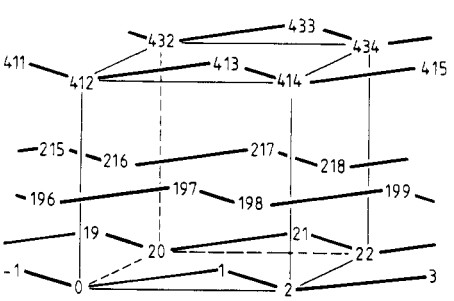

Figure 1. The mapping of the 3D FCC lattice onto the hardware of the DAP. The fine lines show the cubit unit cell. The DAP can be considered as a chain of 4096 processing elements, and each processing element carries the information for one molecule. The numbers of the molecules are given, and the chain is connected at its ends. The chain is shown as the heavy lines.

where a is the length of the FCC unit cell, and the vectors are defined with respect to the three orthogonal axes that define the cubic unit cell.

The equations of motion were integrated using Beeman's algorithm (Beeman 1976), with a time step of 0.01 ps, and were those appropriate for the microcanonical ensemble. The rotational motions were handled using quaternions. Using the inter-molecular potential model described below, the computing processing time to carry out all calculations for all molecules for each time step was about 2.4 s. All calculations associated with the analysis were carried out during the simulations rather than as part of a second separate stage, this being the most efficient method with computers as large and fast as the DAP (Dove and Pawley 1983).

The inter-molecular potential was modelled using a four-site atom–atom Lennard-Jones potential:

$$W = -\sum_{i,j=1}^{4} 4\varepsilon\left[\left(\frac{\sigma}{r_{ij}}\right)^{6} - \left(\frac{\sigma}{r_{ij}}\right)^{12}\right]$$

where r_{ij} is the distance between the ith site of one molecule and the jth site of another. The approach we took in order to obtain values for the potential parameters ε and σ was to vary these parameters in the simulations to obtain agreement at a temperature of 345 K with the two experimental observables of density at low pressures and molecular mean squared displacements (Dolling *et al* 1979, More *et al* 1980). At 345 K the length of the unit cell is 8.85 Å and the mean square displacement is 0.57 Å^2. Initially we tried using the positions of the bromine atoms as the locations of the sites in the potential model, assuming a C–Br bond length of 1.91 Å, but as far as we could tell for all values of ε and σ no OD phase consistent with the two experimental observables exists. It should be noted that for the values suggested by More and Fouret (1980) the model forms a liquid at 345 K. The experience suggested that the model inter-molecular potential was too anisotropic to give orientational disorder below the melting point. The anisotropy could be reduced by including interactions involving the central carbon atoms, but this would give two extra adjustable parameters in the potential function (assuming normal combining rules for interactions between unlike atoms) and would also increase the time required for the simulation calculations. Instead we took a simpler approach and moved the force centres along the C–Br bond towards the carbon atom thus making the molecule more spherical. The parameters σ and ε were adjusted to fit the experimental data using a number of positions of the force centres. Orientational disorder was only obtained for positions less than 80% along the C–Br bond (defining the position of the bromine atom as 100%), and in this study we have considered in detail parameters for 50% and 75% positions of the force centres, which we call the $f = 0.5$ and $f = 0.75$ models respectively. The potential parameters are given in table 1. We consider the latter model probably to resemble the true potential better; the results presented below show that the model with the force centres positioned exactly half-way along the C–Br bond yields a greater degree of randomness in orientations than experimental results suggest. It should be noted that

Table 1. Potential parameters.

Model	σ (Å)	ε (kJ mol^{-1})
$f = 0.5$	4.68	0.4956
$f = 0.75$	4.175	1.9674

the values of σ being large means that the potential minima still lie at distances well outside the C–Br radius in both models, and we stress that the potential models, particularly for $f = 0.75$, are by no means spherical. Electrostatic interactions have not been included.

One of the criticisms often raised against simulation studies is that how closely the model inter-molecular potential resembles the true potential cannot be determined. In this regard we make three points. Firstly, the results presented here and in the following paper on the collective properties of CBr_4 agree reasonably well with experimental data, including the determination of time constants for dynamic properties. Secondly, it is general experience that the behaviour of disordered systems is less dependent on the detailed form of the potential than in ordered systems, so a simple model potential with fitted coefficients might be expected to be adequate. Thirdly, our overall aim in any case is not so much to reproduce Nature in detail, but to identify and study those features of a model that we might expect to be realised in the real system.

4. Orientational variables

In order to analyse the data from the simulations, we need to define variables for the molecular orientations. These can be constructed as symmetry-adapted linear combinations of spherical harmonics. For a tetrahedral molecule, the lowest-order harmonics are for $l = 3$, and we are able to construct seven ($= 2l + 1$) orientational variables. These are given in table 2 in terms of summations over the four C–Br bond vectors, together with the appropriate symmetry species of the variables in the site group O_h. The normalisation constants ensure that the quadrature sum of all seven variables is unity.

In order to relate these orientational variables to actual molecular orientations, we consider two symmetric orientations of a tetrahedron within cubic axes, which are shown

Table 2. Definitions of the seven orientational variables Y_α expressed in terms of the spherical harmonics $Y_{3,m}(\theta, \Phi)$ of the normalised C–Br bond vectors $(x, y, z) = (\sin\theta\cos\Phi, \sin\theta\cos\Phi, \cos\theta)$. The summations are over the four C–Br bonds, and $\Omega_j = (\theta_j, \Phi_j)$.

$$Y_1 = \frac{3(2\pi)^{1/2}\mathrm{i}}{4(35)^{1/2}} \sum_{j=1}^{4} (Y_{3,-2}(\Omega_j) - Y_{3,2}(\Omega_j)) = \frac{3^{3/2}}{4} \sum_{j=1}^{4} x_j y_j z_j$$

$$Y_2 = \frac{3\pi^{1/2}}{2(35)^{1/2}} \sum_{j=1}^{4} Y_{3,0}(\Omega_j) = \frac{3(5)^{1/2}}{40} \sum_{j=1}^{4} (5z_j^3 - 3z_j)$$

$$Y_3 = \frac{3\pi^{1/2}}{8(35)^{1/2}} \sum_{j=1}^{4} [5^{1/2}(Y_{3,-3}(\Omega_j) - Y_{3,3}(\Omega_j)) - 3^{1/2}(Y_{3,-1}(\Omega_j) - Y_{3,1}(\Omega_j))] = \frac{3(5)^{1/2}}{40} \sum_{j=1}^{4} (5x_j^3 - 3x_j)$$

$$Y_4 = \frac{-3^{1/2}\pi\mathrm{i}}{8(35)^{1/2}} \sum_{j=1}^{4} [5^{1/2}(Y_{3,-3}(\Omega_j) + Y_{3,3}(\Omega_j)) + 3^{1/2}(Y_{3,1}(\Omega_j) + Y_{3,-1}(\Omega_j))] = \frac{3(5)^{1/2}}{40} \sum_{j=1}^{4} (5y_j^3 - 3y_j)$$

$$Y_5 = \frac{3(2\pi)^{1/2}}{4(35)^{1/2}} \sum_{j=1}^{4} (Y_{3,2}(\Omega_j) + Y_{3,-2}(\Omega_j)) = \frac{3^{3/2}}{8} \sum_{j=1}^{4} z_j(x_j^2 - y_j^2)$$

$$Y_6 = \frac{-3\pi^{1/2}}{8(35)^{1/2}} \sum_{j=1}^{4} [3^{1/2}(Y_{3,-3}(\Omega_j) - Y_{3,3}(\Omega_j)) + 5^{1/2}(Y_{3,-1}(\Omega_j) - Y_{3,1}(\Omega_j))] = \frac{3^{3/2}}{8} \sum_{j=1}^{4} x_j(y_j^2 - z_j^2)$$

$$Y_7 = \frac{-3\pi^{1/2}\mathrm{i}}{8(35)^{1/2}} \sum_{j=1}^{4} [3^{1/2}(Y_{3,3}(\Omega_j) + Y_{3,-3}(\Omega_j)) - 5^{1/2}(Y_{3,1}(\Omega_j) + Y_{3,-1}(\Omega_j))] = \frac{3^{3/2}}{8} \sum_{j=1}^{4} y_j(z_j^2 - x_j^2)$$

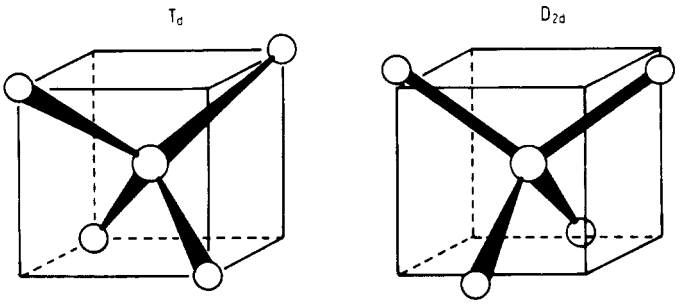

Figure 2. Two possible orientations of a tetrahedron in an octahedral site. The point group symmetries are given.

in figure 2. For the two possible T_d orientations, $Y_1 = \pm 1$ and all other variables are zero. There are six possible D_{2d} orientations, with only variables of T_{2u} symmetry having non-zero values (see table 2). In fact the T_{2u} variables can be considered as a vector, (Y_5, Y_6, Y_7), with two zero components and the third equal to ± 1, thereby characterising the six possible D_{2d} orientations. It should be noted that in the low-temperature phase it is these D_{2d} orientations that freeze into the crystal structure with only a small lattice distortion, with diagonal chains of molecules of the same orientations and including all six components. In the spin or Frenkel model of the disorder in CBr_4 (see, e.g., Coulon and Descamps 1980) it is assumed that each molecule exists in any one of these six orientations in a random manner. In this model a random distribution of the molecules over all six orientations would give

$$\langle Y_1^2 \rangle = \langle Y_2^2 \rangle = \langle Y_3^2 \rangle = \langle Y_4^2 \rangle \simeq 0 \qquad \langle Y_5^2 \rangle = \langle Y_6^2 \rangle = \langle Y_7^2 \rangle \simeq \tfrac{1}{3}.$$

A description of the orientational behaviour can also be made in terms of the probability distribution function of C–Br bonds, $P(\Omega)$, where $\Omega = (\theta, \Phi)$. Formally this can be given as an expansion in Kubic harmonics (Press and Huller 1973):

$$P(\Omega) = \frac{1}{4\pi}\left(1 + \sum_{l=2}^{\infty} c_l K_l(\Omega)\right)$$

where terms with odd l are absent by symmetry, $K_0 = 1$ and K_2 is also absent. The coefficients c_l are equal to $\langle K_l \rangle$, and the functions $K_l(\Omega)$ up to $l = 10$ are given in table 3. For a purely random distribution all values of $\langle K_l(\Omega) \rangle$ (except of course for $l = 0$) will be zero.

Table 3. The Kubic harmonic functions $K_l(\Omega)$ for cubic O_h symmetry. $Q = x^4 + y^4 + z^4$ and $S = x^2y^2z^2$, where $x = \sin\theta\cos\Phi$, $y = \sin\theta\sin\Phi$, $z = \cos\theta$ and $\Omega = (\theta, \Phi)$.

$K_0(\Omega) = 1$
$K_4(\Omega) = \frac{1}{4}(21)^{1/2}(5Q - 3)$
$K_6(\Omega) = \frac{1}{8}(\frac{13}{2})^{1/2}(462S + 21Q - 17)$
$K_8(\Omega) = \frac{1}{32}(561)^{1/2}(65Q^2 - 208S - 94Q + 33)$
$K_{10}(\Omega) = \frac{1}{64}(\frac{4199}{2})^{1/2}(7106QS + 187Q^2 - 3190S - 264Q + 85)$

5. Results

5.1. Thermodynamic properties

Various thermodynamic quantities of interest were calculated from the simulations for both potential models, and the results are given in table 4. The pressure P was evaluated from the virial in the normal manner, and long-range effects (beyond the second shell of neighbours) were included by integration over an effective continuum. The internal energy of the monoclinic phase has been measured as 60.2 kJ mol^{-1} (Wagman *et al* 1982), and it can be seen from table 4 that this value agrees with the internal energy calculated in the $f = 0.75$ model to within 10%. The heat capacity at constant volume, C_v, was calculated from the temperature fluctuations. This has been measured for CBr_4 by Marshall *et al* (1956), who obtained a value of 48.1 ± 2.5 J mol^{-1} K^{-1}. The value calculated for the $f = 0.75$ model differs from this experimental value by only 2.4 standard deviations, whereas the value for the $f = 0.5$ model is in greater disagreement. No other quantities (besides the mean square displacement $\langle u^2 \rangle$, which was used to fit the potential parameters) have been measured.

Table 4. Various thermodynamic quantities of the OD phase of CBr_4 as determined in the present study for the two potential models used. Where appropriate a standard deviation is given, which represents the deviation of the ensemble average over the total number of configurations analysed.

Quantity	Values		Unit
	$f = 0.5$ model	$f = 0.75$ model	
Total energy	−21.087	−67.616	kJ mol^{-1}
Temperature	344.6 ± 1.8	343.2 ± 2.0	K
Potential energy	−29.686 ± 0.044	−76.181 ± 0.049	kJ mol^{-1}
Pressure	−0.020 ± 0.027	−0.024 ± 0.035	kbar
Heat capacity (C_v)	36.5	42.1	J mol^{-1} K^{-1}
Mean square displacement ($\langle U^2 \rangle$)	0.560 ± 0.018	0.559 ± 0.015	$Å^2$
Mean square force $\langle F^2 \rangle$	1306 ± 36	3957 ± 68	g $Å^2$ s^{-4}
Mean square torque $\langle \tau^2 \rangle$	37.5 ± 1.1	706 ± 14	g $Å^2$ s^{-4}

It is not surprising that the two models give different results for the binding energies. The forces and torques are greater for the more anisotropic model, since the molecule in the $f = 0.5$ model is much softer.

5.2. Molecular orientations

Mean squared values of the orientational variables $\langle Y_\alpha^2 \rangle$ and the average values of the Kubic harmonic functions are given in table 5. We also calculated $\langle K_3(\Omega) \rangle$ in order to check that the simulations did give a truly disordered system, and the resultant zero value confirmed this. The feature immediately evident from the values of the orientational variables given in table 5 is that they do not appear to correspond to the values expected for the D_{2d} spin-variable model. It seems that the values of the orientational variables

Table 5. Averages of orientational variables and Kubic harmonic amplitudes for the OD phase of CBr_4 at 345 K. For comparison the expected values for only T_d and D_{2d} orientations and for complete uniform disorder are given. Experimentally determined values are also given (column A, More *et al* (1980); column B, Press *et al* (1979)); the values of the orientational variables Y_1^2 etc were derived from the values of K_4 and K_6. Note that $Y_2^2 = Y_3^2 = Y_4^2$ and $Y_5^2 = Y_6^2 = Y_7^2$.

Quantity	Calculated for $f = 0.5$ model	Calculated for $f = 0.75$ model	Expected for T_d orientation	Expected for D_{2d} orientation	Expected for uniform distribution	Experimental measurements A	Experimental measurements B
Y_1^2	0.125	0.070	1.0	0.0	0.143	0.008	0.197
Y_2^2	0.149	0.155	0.0	0.0	0.143	0.106	0.044
Y_5^2	0.143	0.155	0.0	$\frac{1}{3}$	0.143	0.225	0.224
K_4	0.017	0.052	−1.528	−0.255	0.0	0.06 ± 0.02	−0.37 ± 0.09
K_6	−0.008	−0.077	2.266	−1.700	0.0	−0.83 ± 0.07	−0.57 ± 0.08
K_8	0.001	0.013	0.877	0.621	0.0	0.14 ± 0.14	0.85 ± 0.17
K_{10}	−0.001	−0.009	−2.979	−0.931	0.0	—	—

correspond to the existence of a wider range of orientations. However, the non-zero values for the Kubic harmonic coefficients given in table 5 and the fact that the values of the set of $\langle Y_\alpha^2 \rangle$ are not all equal show that this range of orientations does not correspond to a uniform (i.e. spherically symmetric) distribution, although it is clear that the distribution in the $f = 0.5$ model is more nearly uniform.

We have calculated the C–Br bond orientational distribution function (which we denote the C_3 ODF), and this is shown for both potential models in figure 3. The first point that we make is that the distribution for $f = 0.75$ is in reasonable agreement with that obtained experimentally from fitted values of $\langle K_4 \rangle$ and $\langle K_6 \rangle$ only (Dolling *et al* 1979). The main feature is the strong lobe in the 110 direction which is broadened in the 001 plane, and this is consistent with the experimentally determined distribution (Dolling *et al* 1979). It is this lobe that is evidence for the D_{2d} spin model, as it is consistent with two peaks at $(2^{1/2}, 1, 0)$ and $(1, 2^{1/2}, 0)$ which are librationally broadened and hence unresolved. It is clear however that the distribution never deviates from that corresponding to a purely uniform distribution by much more than 50%.

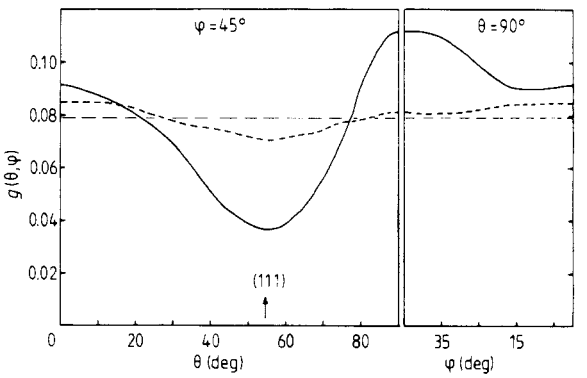

Figure 3. The C–Br bond orientation distribution function $g(\theta, \Phi)$ as a function of polar angles. The full and broken curves denote the $f = 0.75$ and $f = 0.5$ models respectively. The broken straight line at $1/4\pi$ is for the totally random distribution.

There are, however, significant differences between the ODF calculated here and that obtained experimentally, which we attempt to explain. The first is that the distribution along 001 is a maximum in the simulations but a minimum in the experimentally determined ODF. A second discrepancy is that although both the simulation and experimental data give a minimum in the 111 direction, the value of the ODF for this direction obtained from experiment is negative whereas it is only half the random value in the simulation. Of course, the negative regions are unphysical and probably result from the fact that only the first two coefficients ($l = 4$ and 6) could be accurately determined. It would appear then that the neglect of higher-order terms can give rise to errors that are of the same size as the distribution function, so perhaps the discrepancies in the 001 direction are not critical. It is worth noting that part of the observed peak in the 001 direction is constructed from Kubic harmonics for $l > 6$. Thus we conclude that in view of the uncertainties outlined above the behaviour observed in the simulations is in accord with that determined experimentally, particularly in that both ODFs peak along 110.

A second point to be noted from figure 3 is that the more isotropic model ($f = 0.5$) shows a much more uniform distribution of orientations, consistent with the values of $\langle K_l \rangle$ given for this model in table 5.

In addition, we also calculated the ODF for the S_4 molecular symmetry directions, and this is given in figure 4. The important point that this shows is that this distribution is inconsistent with that expected for a pure D_{2d} spin model. In the latter case we should expect peaks of equal strength along 001 and 110, with minima along 111 and elsewhere. Instead the ODF consists of peaks along 110 elongated towards a saddle point at 111 with minima close to 001.

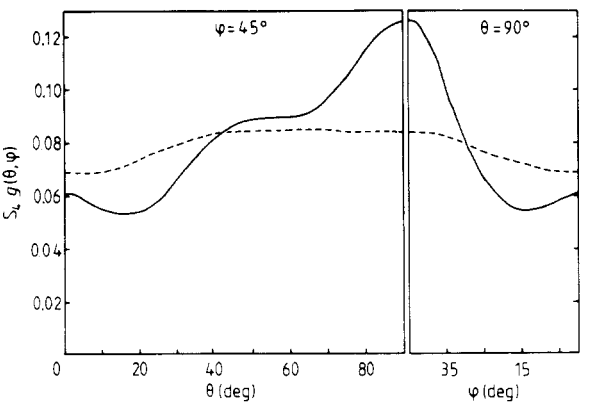

Figure 4. The S_4 ODF as a function of polar angles. The full and broken curves denote the $f = 0.75$ and $f = 0.5$ models respectively.

5.3. Correlations between neighbouring molecules

In order to study aspects of the correlations between the orientations of neighbouring molecules we have calculated the distribution functions for C . . . C and Br . . . Br distances, separating the distribution functions for nearest and next-nearest neighbours. The C . . . C distribution functions are shown in figure 5 and are more or less of the expected form, with peaks corresponding to the mean relative lattice positions which are broadened according to the large mean squared displacements (see table 4). The distribution functions for the two models are very similar, the only differences being that the centroids of the distribution functions are slightly shifted to lower distances in the $f = 0.5$ model, which reflects the softer potential in that case.

Whereas the C . . . C distribution functions are sensitive to relative displacements, the Br . . . Br distribution functions are primarily determined by relative orientations of neighbouring molecules. The distribution functions obtained are given in figure 6. Two features are immediately striking; the first is that for the nearest-neighbour pairs the distributions are different for the two models, and the second is that there is significant structure on the nearest-neighbour distribution functions for the $f = 0.75$ model, which suggests the existence of strong short-range orientational correlations due to steric hindrance. One important feature is the apparent maximum at 4.3 Å with the rapid decay at lower distances. This is close to the expected contact distance $2^{1/6}\sigma = 4.67$ Å. If we consider two next-nearest-neighbour molecules with the D_{2d} orientation with C–Br bonds pointed at each other, there are two possible relative orientations, with parallel

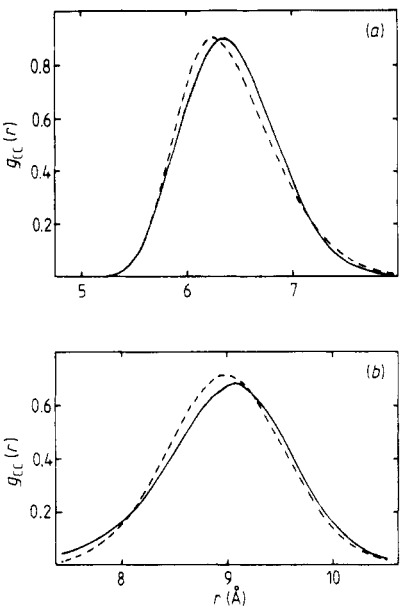

Figure 5. C . . . C radial distribution functions for (*a*) nearest neighbours and (*b*) next-nearest neighbours. The full and broken curves denote the $f = 0.75$ and $f = 0.5$ models respectively.

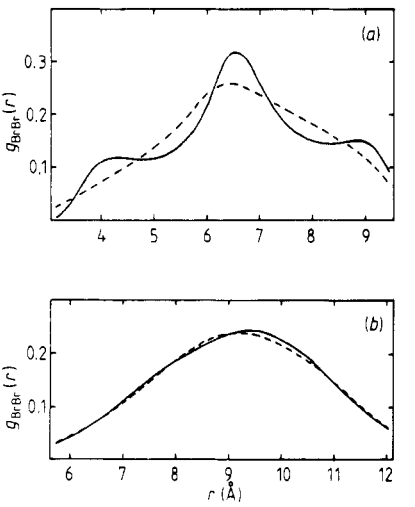

Figure 6. Br . . . Br radial distributions functions for (*a*) nearest neighbours and (*b*) next-nearest neighbours. The full and broken curves denote the $f = 0.75$ and $f = 0.5$ models respectively.

and perpendicular in-plane D_{2d} axes. For molecules on the lattice sites, these give contact distances of 3.47 and 3.43 Å respectively. It is thus clear that steric hindrance does forbid these relative orientations, as assumed by Coulon and Descamps (1980) in their analysis of diffuse scattering. The second peak in the distribution lies at a distance of 6.53 Å and corresponds closely to the mean nearest-neighbour C . . . C distance, and thus represents the mean distance between points on two shells surrounding the molecule centres.

5.4. Single-particle dynamics

In order to study the dynamical behaviour of single molecules we have calculated the following three auto-correlation functions:

$$C_{vv}(t) = \langle \boldsymbol{v}(t) \cdot \boldsymbol{v}(0) \rangle / \langle |\boldsymbol{v}(0)|^2 \rangle$$

$$C_{\omega\omega}(t) = \langle \boldsymbol{\omega}(t) \cdot \boldsymbol{\omega}(0) \rangle / \langle |\boldsymbol{\omega}(0)|^2 \rangle$$

$$M_{\alpha\alpha}(t) = \langle Y_\alpha(t) Y_\alpha(0) \rangle / \langle Y_\alpha(0)^2 \rangle$$

where $\boldsymbol{v}(t)$ and $\boldsymbol{\omega}(y)$ are the linear and angular velocities respectively at time t and the set of $Y_\alpha(t)$ have been defined in the preceding section (table 2). The angle brackets denote averaging over all molecules and over time.

The two velocity auto-correlation functions $C_{vv}(t)$ and $C_{\omega\omega}(t)$ are shown in figure 7, and display many features in common with other orientationally disordered crystals. $C_{vv}(t)$ is similar in appearance for both potential models, the only difference being that the first minimum for the $f = 0.5$ model is at twice the time for that for the $f = 0.75$ model. This is consistent with the fact that the potential for the $f = 0.5$ model is softer.

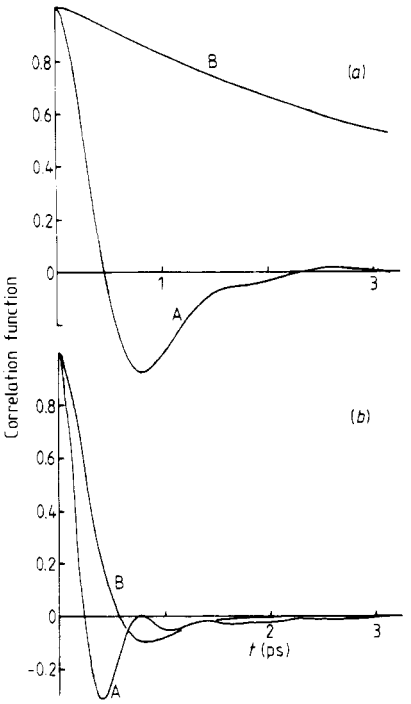

Figure 7. Velocity auto-correlation functions for (*a*) the $f = 0.5$ model and (*b*) the $f = 0.75$ model. Curves A and B denote translational and rotational velocities.

The Fourier transforms of $C_{vv}(t)$ are shown in figure 8. We highlight one important feature observed here particularly for the $f = 0.75$ model. The Fourier transform of $C_{vv}(t)$ is identical to the one-phonon density of states, and in the low-frequency limit where there is little dispersion of the acoustic modes this density of states is generally approximately parabolic in frequency. However, in the present case this is not so, and the dependence is instead roughly linear. A similar situation was found for SF_6 (Dove and Pawley 1983). We cite the MDS study of the ordered and disordered phases of bicyclo-octane by Neusy *et al* (1984) in order to demonstrate that this is not an artefact of the small simulation sample sizes and the limited range of wave-vectors available in simulations. Using samples smaller than used here by a factor of 16, these authors found that the ordered phase showed parabolic and the disordered phase linear limiting behaviour. Thus one must conclude that this linear density of states is an intrinsic property of orientationally disordered crystals which can only arise through a coupling of the acoustic phonons and the molecular orientational disorder. The task of giving a theoretical description for this behaviour remains. Unfortunately it is not obvious how this feature can be demonstrated experimentally, as the low-frequency behaviour will in general be masked by the reorientational behaviour described below.

The angular velocity auto-correlation function $C_{\omega\omega}(t)$ shows a dramatic model dependence. $C_{\omega\omega}(t)$ for the $f = 0.5$ model corresponds to lightly damped rotation, with a lifetime of 3.2 ps. On the other hand, $C_{\omega\omega}(t)$ for the $f = 0.75$ model is much more strongly

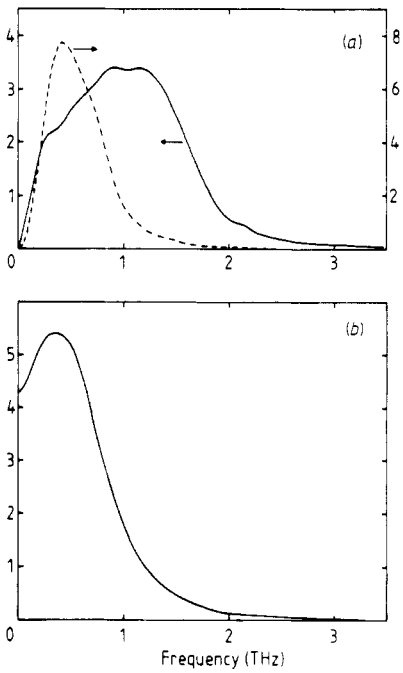

Figure 8. (*a*) Power spectra associated with the linear velocity auto-correlation functions. The full and broken curves denote the $f = 0.75$ and $f = 0.5$ models respectively, and scales are indicated by the left- and right-hand axes respectively. (*b*) The power spectrum associated with the angular velocity auto-correlation function for the $f = 0.75$ model. Note that the vertical axes are drawn to scale relative for each of the three curves, but absolute values are arbitrary.

damped and goes negative after only 0.57 ps. This is much more indicative of strongly hindered reorientational motion than 'free' rotation. The power spectrum for this model is shown in figure 8. The significant non-zero value for zero frequency is related to the existence of a large rotational diffusion constant.

The correlation functions associated with three independent orientational variables $M_{\alpha\alpha}(t)$ ($\alpha = 1$, 2 and 5) are shown in figure 9. As for $C_{\omega\omega}(t)$ there is a significant dependence on the potential model. In the $f = 0.5$ model the greater rotational mobility of the molecules means that the orientational correlations all decay relatively rapidly (within 1 ps) and that the three different symmetry types more or less all display the same behaviour. This is consistent with the fact that the seven values of $\langle Y_\alpha^2 \rangle$ are not very different (table 5). On the other hand, the $f = 0.75$ model, which has greater anisotropy, shows different behaviour for the different symmetry types. The A_{2u} correlation function $M_{11}(t)$ decays rapidly and does not differ much between models. The T_{1u} correlation function $M_{22}(t)$ and the T_{2u} function $M_{55}(t)$ are both longer-lived and are approximately of the form $\exp(-t/\tau_{\alpha\alpha})$. The characteristic times are $\tau_{22} \simeq 1.9$ ps and $\tau_{55} \simeq 2.5$ ps, which are in close agreement with a value for single-particle reorientational dynamics of 2.2 ps suggested from inelastic neutron scattering data (More *et al* 1984). It is significant that the longest-lived orientational correlation functions are those for the T_{2u} orientational variables, which are those that correspond to D_{2d} ordering and that order in the low-temperature phase.

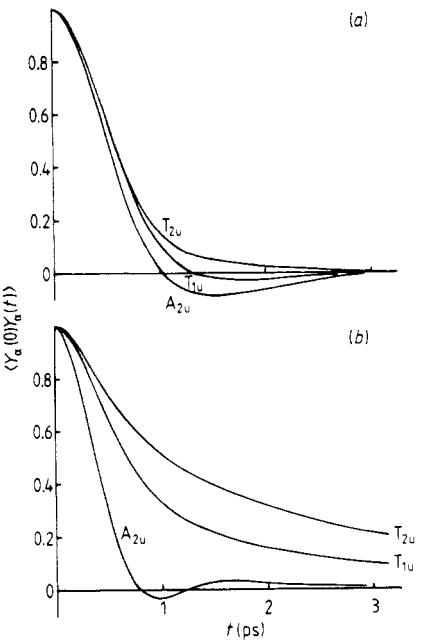

Figure 9. Auto-correlation functions for the orientational variables for (*a*) the $f = 0.5$ model and (*b*) the $f = 0.75$ model. The three curves in each case are for the $A_{2u}(\alpha = 1)$, $T_{1u}(\alpha = 2, 3, 4)$ and $T_{2u}(\alpha = 5, 6, 7)$ variables.

6. Information from computer graphics

Recent developments in computer graphics have enabled the realistic visual representation of molecules to become a routine operation. These techniques can be used in conjunction with computer simulations to give visual images of the dynamics of disordered crystals. The trajectories of the ensemble of molecules that are generated by the simulations can be used to produce movies of their motions; the techniques for doing this and the type of information obtainable are described elsewhere (Dove *et al* 1986a). This technique has been used to complement simulation studies of the disordered phase of SF_6 (Dove and Pawley 1983, 1984) in order to study the reorientational dynamics of molecules. We have produced movie films showing planes of CBr_4 molecules for the $f = 0.75$ model, and describe here the relevant information that they have given.

The complex orientational behaviour suggested by the results given in § 5.2 was confirmed by the graphic representations. No average well defined symmetric orientations were observed, and instead many different orientations corresponding to a continuous distribution were seen. It was necessary to use the formal techniques of analysis outlined in § 5.2 to show that the distribution in orientations is not in fact completely uniform. The rotational motions were of two kinds. The primary motion was diffusion-like, with the molecules librating about slowly varying orientations. However, this motion was occasionally interrupted by the second type of motion, which corresponds more to free spinning for a few complete (i.e. 360°) rotations about an apparently arbitrary axis. These two types of motions can be differentiated by the observation that rotational diffusion corresponds to a continuous variation of the orientation of the

rotation axis, whereas for free-rotational motion the orientation of this axis remains approximately (although of course not exactly) constant in time. The transition from diffusion to free rotation appears to be coupled to local density fluctuations; the surrounding cage of molecules needs to expand in order to give the rotating molecule the space it needs. Once a molecule is set spinning, its large moment of inertia (compared, say, with that for SF_6 or an ammonium ion) means that it will not be stopped immediately. In the paper of Dove *et al* (1986a), a coloured plate is presented that shows the complex rotational motion of a single CBr_4 molecule.

Finally, another feature observed in the films was that the rotational motions of the CBr_4 molecules are affected by steric hindrance, as suggested by the results of § 5.3. It was clear that the molecules moved to avoid close Br . . . Br contacts, this clearly being the origin of the rotational diffusion. One particularly interesting feature was that occasionally neighbouring molecules became locked into cog–wheel-type correlated reorientational motions.

7. Discussion

7.1. Potential model

Of the two model inter-molecular potential functions that we used, it is clear that the $f = 0.75$ model is by far the more realistic representation of the true potential; the $f = 0.5$ model was too isotropic, giving approximately uniform orientations and free-molecular rotations. We recall that the $f = 0.75$ model was parametrised to reproduce the observed unit cell dimension and mean squared centre-of-mass displacement at atmospheric pressure and 345 K. The test of any potential model is how well it reproduces other experimental data that were not incorporated into the development of the model. There are three such independent tests reported in this study. The first is the agreement between the experimental and calculated internal energy and specific heat (§ 5.1), the second is the reasonable agreement between the features of the C–Br bond orientational distribution function calculated here and obtained experimentally, particularly in view of the difficulties in extracting this function from diffraction data (§ 5.2), and the third is the good agreement of the single-molecule reorientational correlation times obtained from experiment and simulation (§ 5.4). In addition we cite two comparisons between quantities determined from both experiments and simulations from our work on the collective properties of CBr_4 (Dove and Lynden-Bell (1986), the following paper). The first is that there is reasonable agreement between the frequencies of the long-wavelength acoustic modes calculated in the simulation and measured by inelastic neutron scattering (More and Fouret 1980), and the simulations yield quasi-elastic scattering from collective motions with longer correlation times than for the single-molecule reorientational dynamics as observed experimentally (More *et al* 1984).

The fact that this potential was parametrised on a limited amount of experimental data but yet is able to reproduce a wide variety of other properties, static and dynamic, suggests that we can have confidence in its use as a realistic model potential. Of course, the simplicity of the form of the model potential will mean that fine detail will not be reproduced. However, the general features of the disordered phase of CBr_4 that are characteristic of OD crystals are quantitatively as well as qualitatively reproduced by the model potential we have used here, and it is these features in which we are primarily interested. Accordingly, confident in the realism of our $f = 0.75$ potential, we have used

simulations to study aspects of rotation–translation coupling and collective dynamics in CBr_4, the results being presented in the following paper.

7.2. Orientational order

The main conclusion concerns the orientational order. It has been assumed by other workers, and particularly reinforced by Descamps (1984), that CBr_4 in its disordered phase has the molecules lying in long-lived discrete spin-like orientations, with occasional reorientations between different discrete orientations. These are the six D_{2d} orientations. However, this study has found this model to be too severe; instead there exist a wider range of orientations, but still with an anisotropic distribution, with continuous rotational diffusion rather than jump-diffusion being the characteristic dynamic behaviour.

The experimental evidence for the discrete orientation model is mainly the C–Br bond orientation distribution function, and indirect support for the D_{2d} spin model comes from the calculations of anomalous diffuse scattering by Coulon and Descamps (1980). In their calculations they assumed that the molecules could only have D_{2d} orientations, and that the atoms could be treated as hard spheres. The anomalous diffuse scattering could be explained as a result of steric hindrance forbidding certain relative orientations. The agreement with the experimental results is certainly impressive. However, Dolling *et al* (1979) have measured the diffuse scattering for both liquid and polycrystalline disordered CBr_4, showing that there are few differences between the two phases. Since the D_{2d} model is not at all appropriate for the liquid, one can conclude that the primary origin of the diffuse scattering lies in the short-range orientational correlations caused by steric hindrance with little regard to the absolute orientations of the molecules. This is consistent with the results of this study, and such steric hindrance has been observed in the simulations (§ 5.3). In addition, as well as the anomalous diffuse scattering there is a lot of diffuse scattering that is due to single-molecule disorder, and this has been explained on a qualitative basis assuming uniform distribution of the molecular orientations (Dolling *et al* 1979).

On the other hand, there is strong evidence in the simulations of incipient ordering of the D_{2d} orientations as a precursor to the low-temperature phase. We have shown that the orientational correlation functions associated with these orientations (i.e. $M_{55}(t)$) are the longest-lived. In addition, our study of the collective properties of CBr_4 (Dove and Lynden-Bell 1986) has shown that there is a very strong coupling between these orientational variables and the acoustic phonons, and the calculated scattering from these modes shows that the collective correlations for these variables are long-lived.

8. Conclusions

A computer simulation model for the OD phase of CBr_4 has been developed. Calculations of thermodynamic properties, single-particle orientational distribution functions, neighbour correlations and single-particle dynamics have been performed, and, where possible, compared with experimental data. In all cases agreement is satisfactory, which shows that the model gives a realistic simulation of CBr_4. The model shows that the orientational disorder and the rotational motions are more complex than previously thought, although expected precursor effects of the low-temperature ordered phase are observed.

In order to study precursor effects it is necessary to consider collective properties.

Confident of the realism of the model inter-molecular potential, we have studied the coupling between orientational variables and the acoustic phonons as a function of wave-vector, and the collective excitation. The results are presented in the following paper.

Acknowledgments

The author thanks Dr R M Lynden-Bell for many helpful discussions. Financial support was provided by SERC (UK). Support of the Queen Mary College Computer Centre is also gratefully acknowledged.

References

Beeman D 1976 *J. Comput. Phys.* **20** 130
Coulon G and Descamps M 1980 *J. Phys. C: Solid State Phys.* **13** 2947
Descamps M 1984 *J. Physique* **45** 587
Dolling G, Powell B M and Sears V F 1979 *Mol. Phys.* **37** 1859
Dove M T, Fincham D and Hubbard R 1986a *J. Mol. Graphics* **4** 79
Dove M T and Lynden-Bell R M 1986 *J. Phys. C: Solid State Phys.* **19**
Dove M T and Pawley G S 1983 *J. Phys. C: Solid State Phys.* **16** 5969
—— 1984 *J. Phys. C: Solid State Phys.* **17** 6581
Dove M T, Pawley G S, Dolling G and Powell B M 1986b *Mol. Phys.* **57** 865
Huller A and Press W 1979 *The Plastically Crystalline State* ed. J N Sherwood (Chichester: Wiley)
Lynden-Bell R M, Klein M L and McDonald I R 1984 *Z. Phys.* B **54** 325
Lynden-Bell R M, McDonald I R and Klein M L 1983 *Mol. Phys.* **48** 1093
Marshall J G, Staveley L A K and Hart K R 1956 *Trans. Faraday Soc.* **52** 19
More M, Baert F and Lefebvre J 1977 *Acta Crystallogr.* B **33** 3681
More M and Fouret R 1980 *Discuss. Faraday Soc.* **69** 75
More M, Lefebvre J and Hennion B 1984 *J. Physique* **45** 303
More M, Lefebvre J, Hennion B, Powell B M and Zeyen C M E 1980 *J. Phys. C: Solid State Phys.* **13** 2833
Neusy E, Nosé S and Klein M L 1984 *Mol. Phys.* **52** 269
Pawley G S and Dove M T 1983 *Helv. Phys. Acta* **56** 583
Pawley G S and Thomas G W 1982a *Phys. Rev. Lett.* **48** 410
—— 1982b *J. Comput. Phys.* **47** 165
Press W 1981 *Single Particle Rotations in Molecular Crystals, Springer Tracts in Modern Physics* vol 92 (Berlin: Springer)
Press W, Grimm H and Huller A 1979 *Acta Crystallogr.* A **35** 881
Press W and Huller A 1973 *Acta Crystallogr.* A **29** 252
Sherwood J N (ed.) 1979 *The Plastically Crystalline State* (Chichester: Wiley)
Wagman D D, Evans W H, Parker V B, Schumm R H, Halow I, Bailey S M, Churney K L and Nuttall R L 1982 *J. Phys. Chem. Ref. Data* **11** Suppl. 2